


Research Article

Influence of Base Rock Deterioration on Tunnel Bottom Structure Damage under Train Excitation

Zi-Qiang Li ¹, Wei-Wei Huang,² Zheng Li,³ Jian-Wen Feng,⁴ Hang Zhang,⁵ and Qi Li⁶

¹School of Civil Engineering and Architecture, Chongqing University of Science & Technology, Chongqing, China

²Chongqing Key Laboratory of Energy Engineering Mechanics and Disaster Prevention and Reduction, Chongqing University of Science & Technology, Chongqing, China

³Chongqing City Construction Investment (Group) Co., Ltd., Chongqing, China

⁴Architectural Engineering Institute, Chongqing University of Science & Technology, Chongqing, China

⁵Resources and Environment, Chongqing University of Science & Technology, Chongqing, China

⁶College of Architecture and Urban-Rural Planning, Sichuan Agricultural University, Chengdu, China

Correspondence should be addressed to Zi-Qiang Li; lzq1102dd@163.com

Received 5 August 2022; Revised 17 December 2022; Accepted 26 December 2022; Published 4 January 2023

Academic Editor: Xiaofeng Li

Copyright © 2023 Zi-Qiang Li et al. This is an open access article distributed under the Creative Commons Attribution License, which permits unrestricted use, distribution, and reproduction in any medium, provided the original work is properly cited.

In the ground of the preliminary study of the Taihangshan Mountain Tunnel, it was observed that under water-rich conditions, the long rolling of heavy-haul trains would deteriorate the surrounding rock, thereby causing damage to the bottom structure. Combined with data from long-term field monitoring and discrete element analysis, after clarifying the law of bedrock deterioration, the Fuyingzi Tunnel of Zhangtang Railway in China is taken as the research object of fatigue damage. ANSYS Workbench simulation software was used to compare further and analyze the influence of three characteristic deterioration stages of the surrounding rock on the basement structure damage. Based on the results, when the surrounding rock is intact, the basement structure gradually damages and expands from top to bottom, and the structural minimum fatigue life is approximately 76 years. When the surrounding rock is a partial cavity, the damage to the bottom structure intensifies and develops toward the surrounding rock's deterioration position. The minimum fatigue life of the structure is 67 years, which decreases by 11.8%. When the surrounding rock is a cavity and connected, the damage of the bottom structure develops downward to a certain extent, which causes the structural damage at the deterioration position of the surrounding rock to develop in the opposite direction, i.e., from bottom to top. The structural minimum fatigue life is 42 years, which is reduced by 44.7% in the better situation.

1. Introduction

Presently, the heavy-haul railway has become the main development direction of freight transport in the world. Owing to its large axle load, total train load, and traffic volume, the excitation effect of heavy-haul trains on tunnel structure is more significant than that of ordinary railway tunnels stated by Li [1], Li and Shi et al. [2, 3]. When the heavy-haul railway tunnel is under the condition of rich water, the water and soil pressure distribution of the bottom surrounding rock will be significantly affected. In addition, under the rolling vibration of the long-term heavy axle load of heavy-haul trains, the bottom structure will be subjected

to greater train excitation and have a more intense long-term effect than the ordinary railway tunnel; thus, the bottom structure is more prone to fatigue damage. Zuo et al. [4], Niu and Su et al. [5, 6] Based on the investigation of the existing heavy-haul railway tunnel disease, it could be observed that the number of diseases in heavy-haul railway tunnels is 2.5 times that of ordinary railway tunnels, and these diseases are mainly concentrated in the basement structure, such as mud-flushing, base subsidence, and bottom surrounding rock cavitation. The excitation of heavy-haul trains has an important influence on the surrounding rock state and basement structure damage of heavy-haul railway tunnels. Once the overall condition of the basement surrounding

rock deteriorates, the accumulation of time effect will accelerate the occurrence of bottom structure diseases, which significantly influence the operation safety of the heavy-haul railway. Therefore, it is recommended to further study the deterioration mechanism of surrounding rock at the bottom of the tunnel and its influence on the structural failure at the bottom of the tunnel.

A disease of the bottom structure is a manifestation of its damage accumulation, and it also directly influences the fatigue damage of the structure. In this study, 17 tunnels with serious diseases and urgent need for repairs were investigated. The diseased section length of 11 tunnels exceeds 40% of its overall length, and the diseases are mainly concentrated at the bottom of these tunnels, indicating that the disease is universal. The proportion of the length of the heavy-haul line disease section in the length of the tunnel disease section exceeds 50%. The statistical results of the main disease classification and a continuous length of the tunnel bottom are shown in Figure 1.

As shown in Figure 1, in the 17 tunnel survey sections, the cumulative damage length of the tunnel bottom structure reached 6311.7 m, accounting for approximately 74% of the tunnel bottom diseases, and the continuous length of measuring points was primarily concentrated in the range of 3 to 9 m, accounting for approximately 44% of the tunnel bottom damage. Based on comprehensive analysis, the tunnel bottom disease results from a variety of factors, such as the impact of groundwater and the changes in geological conditions; based on field research data, the bottom disease of the heavy-haul railway tunnel is more significant compared with the ordinary passenger and freight line, and the damnification of the basement structure is mainly manifested. The repeated dynamic action of the heavy-haul train is the significant influencing factor of the fatigue damage of the bottom structure of the tunnel; the surrounding rock deterioration and the groundwater erosion also aggravate the development of the bottom structural damage to a certain extent.

Presently, there are some research results on the deterioration and fatigue damage of the surrounding rock of the tunnel bottom structure. In the 1980s, Mandal and Singh [7], and Jeon et al. [8] discussed the strong squeezing effect of tunnels in relatively weak surrounding rocks influenced by large tectonic stress, which gradually increases with the deterioration of surrounding rocks. Hamilton et al. [9] used the shaking table and other simulated scouring test equipment to analyze the hydrodynamic pressure and observed that the mechanical parameters of engineering building materials would be reduced. Ning et al. [10] used a dynamic model to study the decrease in the foundation rock softening coefficient; an increase in softening thickness shortens the life of heavy-haul railway tunnel bottom structures. Gao et al. [11], through the preliminary finite element simulation, concluded that the increase in the basement cavity causes the deterioration of the stress performance of the inverted arch and reduces the life of the inverted structure from 104.42 to 7.08 years. The aforementioned studies on the fatigue life of substructure are mostly based on the assumption that the base rock is intact or defective and that the actual state of the

bedrock lacks the support of the measured data. Therefore, the damage evolution law of the bottom structure lacks objectivity and applicability.

First, based on the change of water-earth pressures in the long-term monitoring of single-line heavy-haul railway tunnels, this study proposes the state change of the basement rock of heavy-haul railway tunnels in a water-rich environment and the degradation and cavity regular pattern of the basement rock are explored by using the discrete element software PFC. Taking the train excitation load measured on-site as the dynamic initial condition, the influence of different deterioration conditions of the basement surrounding rock on the distribution characteristics and the fatigue damage development law of the bottom structure of double-track heavy-haul railway tunnels under the condition of rich water is analyzed by using ANSYS Workbench, which provided a reference for the determination of design parameters and studies on the long-term effect of heavy-haul railway tunnels.

2. Engineering and Long-Term Monitoring Program

2.1. Engineering Overview. Water-earth pressure data collected in the previous study were selected in the Taihangshan Mountain Tunnel of the Watang-Rizhao Railway. The tunnel passes through three surrounding rock grades of Class III, IV, and V, and most areas are in a water-rich environment. The test section is selected in the Class V surrounding rock section, and the lining section is shown in Figure 2.

The Zhangtang Railway is an important third energy channel in China, completed in 2015. The Fuyingzi Tunnel is a long heavy-haul railway tunnel, which adopts the section type of single hole and double lines. The right is the passenger line, and the left is the freight heavy-haul line. Because the excavation section of the double-track tunnel is larger and the stress is uneven during the operation, studies on the effect of the surrounding rock cavity degradation on the fatigue damage of the substructure under the joint action of hydrodynamic pressure and train dynamic load are of great significance. The design lining section of the Fuyingzi tunnel is shown in Figure 3.

After operating the Taihangshan Mountain Tunnel and Fuyingzi Tunnel for seven years, the actual operating axle load of the two heavy-haul railway tunnels was 300 kN, and the opening speed was 80 km/h. The physical correlation between roadway surrounding rock parameters and the structure of the tunnel is selected according to the design specification for the railway tunnel [12], as shown in Table 1.

2.2. Long-Term Monitoring Scheme. At the initial stage of Taihang Mountain tunnel construction, the fiber grating earth and water pressure sensors were buried below the surface of the base rock of the test section, and the measuring points were arranged in a mirror image. To explore the comprehensive influence of groundwater and train dynamic load on the structural characteristics of the bottom position, the measuring points were selected in the arch foot, the

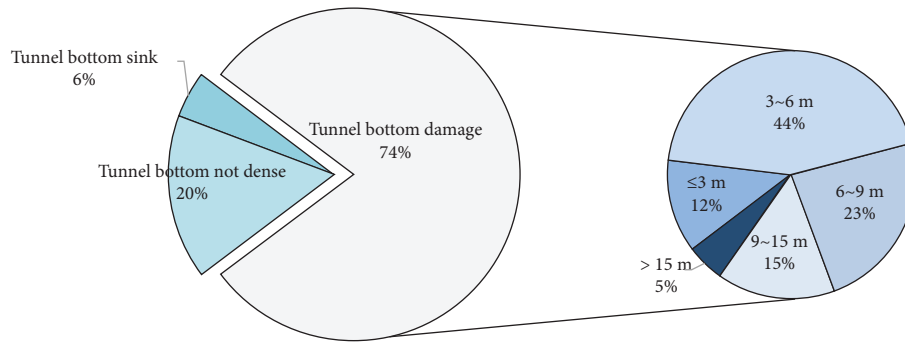


FIGURE 1: Main disease classification and continuous length diagram of tunnel bottom in the investigation section.

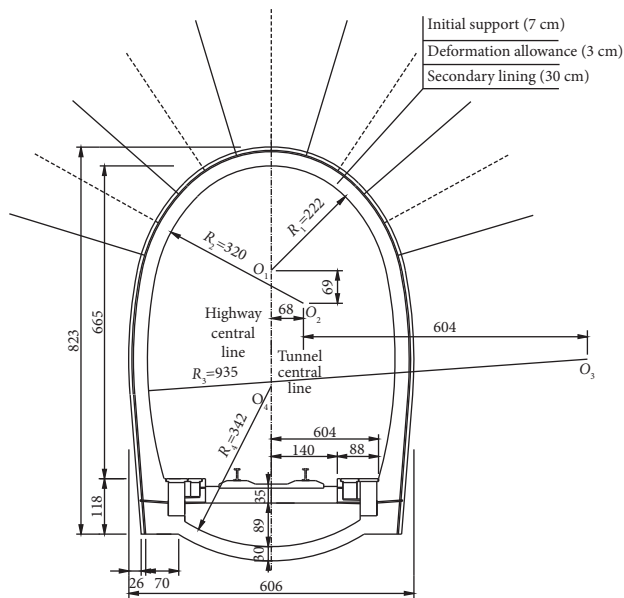


FIGURE 2: Design lining sectional drawing of class V surrounding rock.

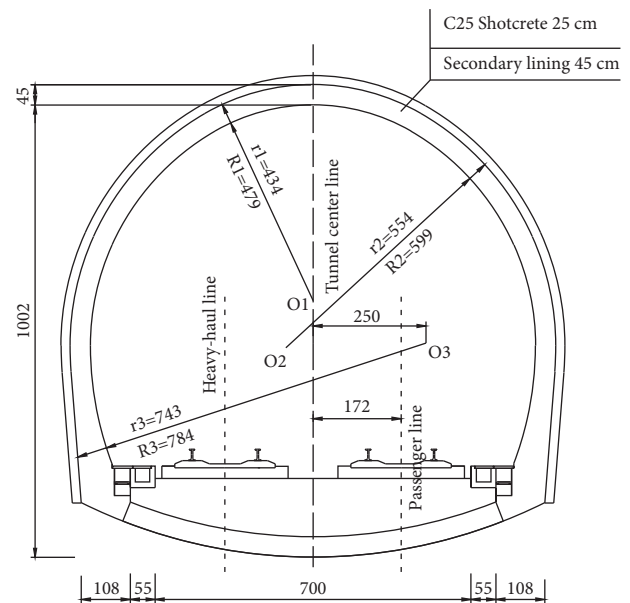


FIGURE 3: Cross section of design lining of double-track heavy-haul railway tunnel (unit: cm).

vertical side ditch, the vertical track, and the middle position of the line. The measuring points are arranged as shown in Figure 4.

The hydrological and geological conditions of the test section of the Taihangshan Mountain Tunnel are intricate; thus, fiber grating water-earth pressure gauges with strong anti-interference ability are selected, as shown in Figure 5. The tunnel has a multiple statically indeterminate structure. Owing to the need for stress accumulation and sensor data stability, the extent of the fiber grating earth pressure (E-1-E-7) is set to 2 MPa, and the range of the fiber grating water pressure (W-1-W-7) is set to 700 kPa, as shown in Figure 5.

After the installation of water-earth pressure sensors, the FBG sensors were connected in series and parallel. All water and earth sensors in the test section of the Taihangshan Mountain Tunnel were networked in the fusion package; finally, a multicore optical cable was introduced into the cable slot.

Owing to the need for real-time monitoring dynamic response, the working environment of the fiber grating

remote transmission system needs to meet the conditions of temperature stability and drying; the main cable was connected to the communication room outside the Taihangshan Mountain Tunnel. Finally, the fiber grating demodulator reads the main optical cable transmission data and displays the change in water-earth pressures in real time in an industrial computer. The industrial computer is connected to the wireless network through the network transmission device to realize remote data acquisition, as shown in Figure 6.

The actual traffic parameters of trains in the Taihangshan Mountain Tunnel are an axle load of 300 kN and a speed of 80 km/h. The monitoring system can trigger data acquisition when heavy-haul trains pass the test section, and the acquisition time interval is 0.01 s.

3. Remote Measurement Results of Water-Earth Pressures

According to the remote data acquisition system, the water-earth pressures of the basement surrounding rock of the

TABLE 1: Surrounding rock parameters and structural parameters of Taihangshan Mountain Tunnel and Fuyingzi Tunnel.

Structure	Elastic modulus (GPa)	Poisson ratio	Unit weight ($\text{kN}\cdot\text{m}^{-3}$)	Cohesion (MPa)	Friction angle ($^{\circ}$)
Surrounding rock	2.0	0.24	20.3	0.012	38
Taihangshan Mountain/Fuyingzi heavy-haul railway Tunnel	Class V				
	Initial support	23.0	0.20	23.0	
	Secondary lining	31.0	0.20	25.0	
	Track bed	33.5	0.20	25.0	
	Inverting fill	28.5	0.20	23.0	
Inverted arch	31.0	0.20	25.0		

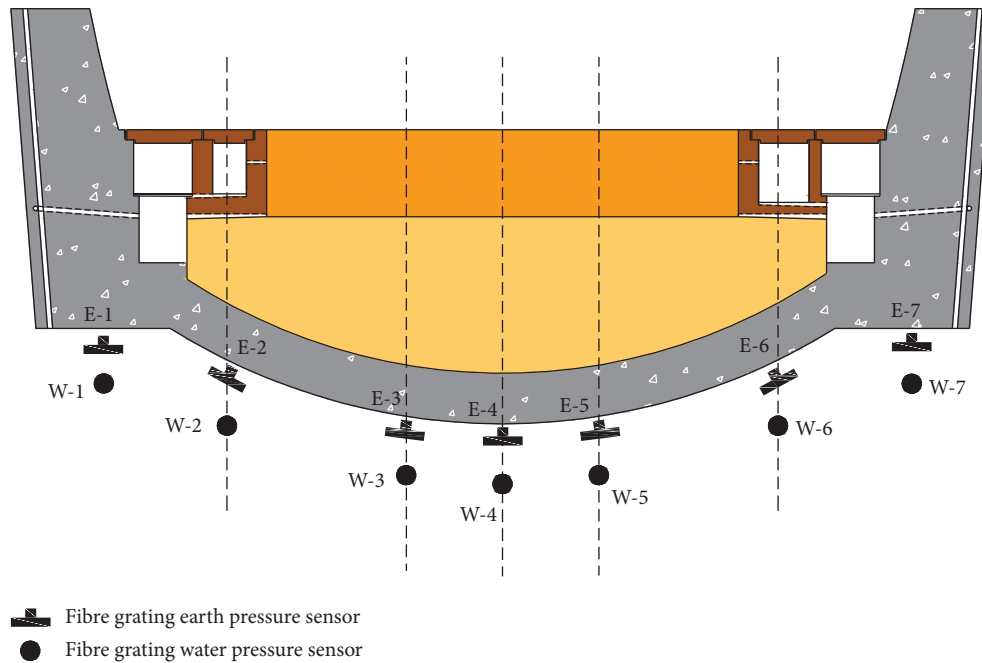


FIGURE 4: Layout of the basement surrounding rock sensor.

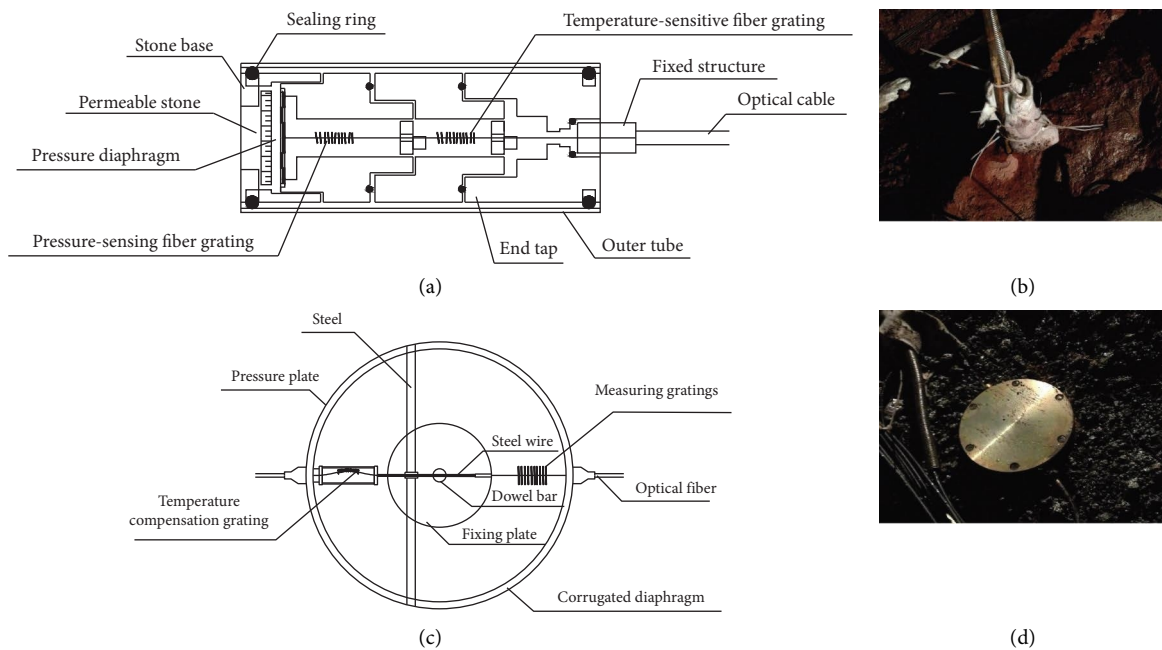


FIGURE 5: Schematic diagram of the installation of fiber grating water-earth pressures sensor: (a) fiber grating water pressure sensor; (b) fiber grating water pressure sensor; (c) fiber grating earth pressure; (d) fiber grating earth pressure.

Taihangshan Mountain Tunnel increase with time, and the growth degrees of water-earth pressures in each characteristic position differ. To explore the correlation between the growth trend of water-earth pressures and the condition of the basement surrounding rock, the water-earth pressures of the basement surrounding rock are analyzed in stages.

3.1. Surface Pressure Long-Term Variation of the Basement Surrounding Rock. As time went on, in accordance with the change of surface pressure of basement rock, long-term variation is divided into five stages (before the operation, one month of operation, six months of operation, one year of operation, and two years of operation) according to the service state, as shown in Figure 7.

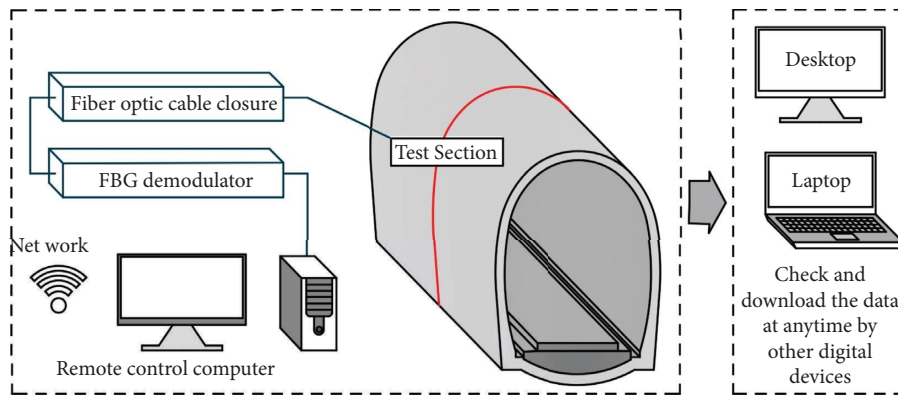


FIGURE 6: Remote monitoring system of the double-track heavy-haul railway tunnel.

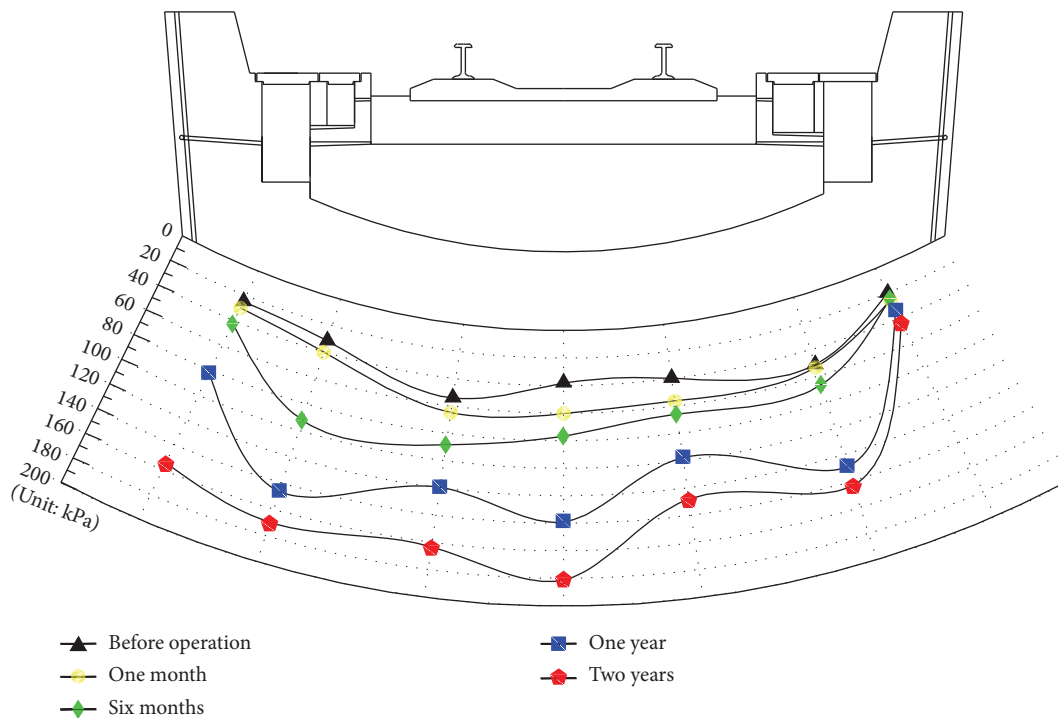


FIGURE 7: Earth pressure change diagram of surrounding rock at the bottom.

As shown in Figure 7, Before the Taihang Mountain Tunnel was put into operation, the earth pressure distribution of the basement rock surface was nearly uniform, and the earth pressure of the left track position and the right groove bottom are 53.99 kPa and 51.35 kPa, respectively, which is significantly greater than that at other positions. This indicates that after the site construction is completed, owing to the influence of geological conditions and construction accuracy, the invert structure, and the basement rock are not fully dense; thus, the symmetrical distribution of the earth pressure is difficult.

After one month, the earth pressure of the basement rock surface increases to varying degrees. Based on the lateral distribution law, the earth pressure at the left amplitude is higher than that at the right amplitude, and the earth pressure at the left orbital position is still the largest, which is

54.52 kPa. It indicates that the dynamic action of the heavy-haul train will lead to the original defects of the base rock increasing with time.

After six months, the earth pressure at the left ditch bottom of the basement rock increases to the maximum, reaching 92.00 kPa, with an increase of 129.48%, indicating that the dynamic action of the train not only aggravates the earth pressure at the vertical position of the load (left track) but also influence the adjacent position. After 1 to 2 years of operation, the earth pressure of the basement rock surface on the left is 2 to 5 times that before the operation, and the increase is much higher than that on the right. The earth pressure at the bottom of the arch reaches the maximum value of 181.10 kPa, which can easily cause the instability of the tunnel basement structure.

3.2. Long-Term Variation of Water Pressure. Section 2.1 shows that the development of base rock defects in the Taihangshan Mountain Tunnel influences the value of earth pressure on its surface. To further study the deterioration law of the bedrock in the water-rich environment, the variation of water pressure at corresponding measuring points was analyzed, and the hydrodynamic pressure corresponding to five characteristic stages (before the operation, one month of operation, six months of operation, one year of operation, and two years of operation) as shown in Figure 8.

As shown in Figure 8, before the operation, the maximum hydrodynamic pressure was 117.35 kPa at the left rail position paralleled to the distribution law of earth pressure. This is because, during the construction process, after inverted arch excavation, there is virtual ballast in the surrounding rock of the basement. If the bottom is not completely cleared, the surrounding rock will not fit closely with the inverted arch, which provides initial conditions for high hydrodynamic pressure.

After one month, the hydrodynamic pressure of every measuring point increased. The water pressure below the left track was the largest because of the development of surrounding rock defects, which is 194.04 kPa, with an increase of 65.4%. After 6 months of operation, the surrounding rock defects because of the track's gradual development under the long-term effect of heavy-haul trains, and the formed cavity maintains the water pressure value of the position the largest, which is 251.79 kPa.

After 1 to 2 years of operation, the water pressure of the left rail measuring point increased from 117.35 to 286.86 kPa. The hydrodynamic pressure at the left ditch and arch bottom of adjacent measuring points increased the most, with an increase of 253.5% at the left ditch bottom and 390.0% at the arch bottom. The increase in hydrodynamic pressure on the left rock surface is larger compared with the right. This reason is that the surrounding rock beneath the left rail is cavitated, which will make the groundwater continuously scour the bedrock under the dynamic action of the heavy-haul train. Deterioration of surrounding rock into loose rock particles provides a channel for the gradual development of defects in this position on both sides (adjacent positions). The longer the time, the more prone to local cavities caused by surrounding rock defects in the basement.

3.3. Relationship between Earth and Water Pressure of the Bedrock. The relationship between hydrodynamic and earth pressures on the basement rock surface under five characteristic stages (before the operation, 1 month, 6 months, 1 year, and 2 years) is shown in Figure 9.

Comparing the relationship between water-earth pressures in Figures 9(a)–9(e), the following conclusions are obtained:

- (1) Before the operation of the tunnel, the left and right amplitude of earth pressure on the surrounding rock surface of the basement is symmetrical, and the water-earth pressures at the left track position are greater than those at other measuring points owing to the local cavity in the construction.

- (2) After one month of operation, the water pressure on the left track of the basement rock surface increases continuously, and the hydrodynamic pressure of adjacent measuring points increases simultaneously. This phenomenon indicates that the local cavity caused by the damage of the basement rock will aggravate the scouring effect when groundwater is abundant and the surrounding rock at the adjacent measuring points becomes unstable. This effect is repeated, which is unfavorable to the basal surrounding rocks.
- (3) After six months of tunnel operation, under the effect of high hydrodynamic pressure at the damaged location, the earth pressure distribution of the basement surrounding rock was uneven, and the high-water-pressure measuring points caused the increase in the earth pressure at the adjacent measuring points. For example, under the long-term action of the hydrodynamic pressure at the left track measuring point, the earth pressure rapidly increases in the left groove and arch bottom. The earth pressure at the left amplitude of the single-track railway tunnel is greater than that at the right amplitude. The damage of the basement surrounding rock intensifies and leads to cavity development, which can easily induce the inverted arch disease. To further explore the long-term variation law of water-earth pressures, the next section uses discrete elements to analyze the deterioration mechanism of surrounding rock and the cavity formation process.

4. Discrete Element Simulation of Basement Surrounding Rock Deterioration

The discrete element model is characterized by non-continuity and nonlinearity, which can effectively simulate the damage and failure mechanisms of rock microscopic medium, and truly reflect the morphological characteristics of surrounding rock particles falling and losing under the effect of groundwater scouring. Therefore, PFC2D discrete element software is used to simulate and analyze the degradation mechanism and cavity formation process of the bedrock under water-rich conditions. Khamitov et al. [13], Liang et al. [14], Ju et al., and Ju and Xing [15, 16] conducted relevant research.

4.1. Calibration of Microscopic Parameters. The process of transforming the macroscopic mechanical parameters of the particles into the microscopic parameters of the corresponding particle model is called calibration. The calibration method usually adjusts the relationship between the experimental parameters and the simulation parameters by comparing the laboratory experiment with the discrete element experiment so that the experimental results obtained by the two are basically consistent. The data comparison between the laboratory experiment and simulation is shown in Figure 10.

According to Figure 10, the overall trend of the stress-strain diagram of the laboratory experiment and the discrete

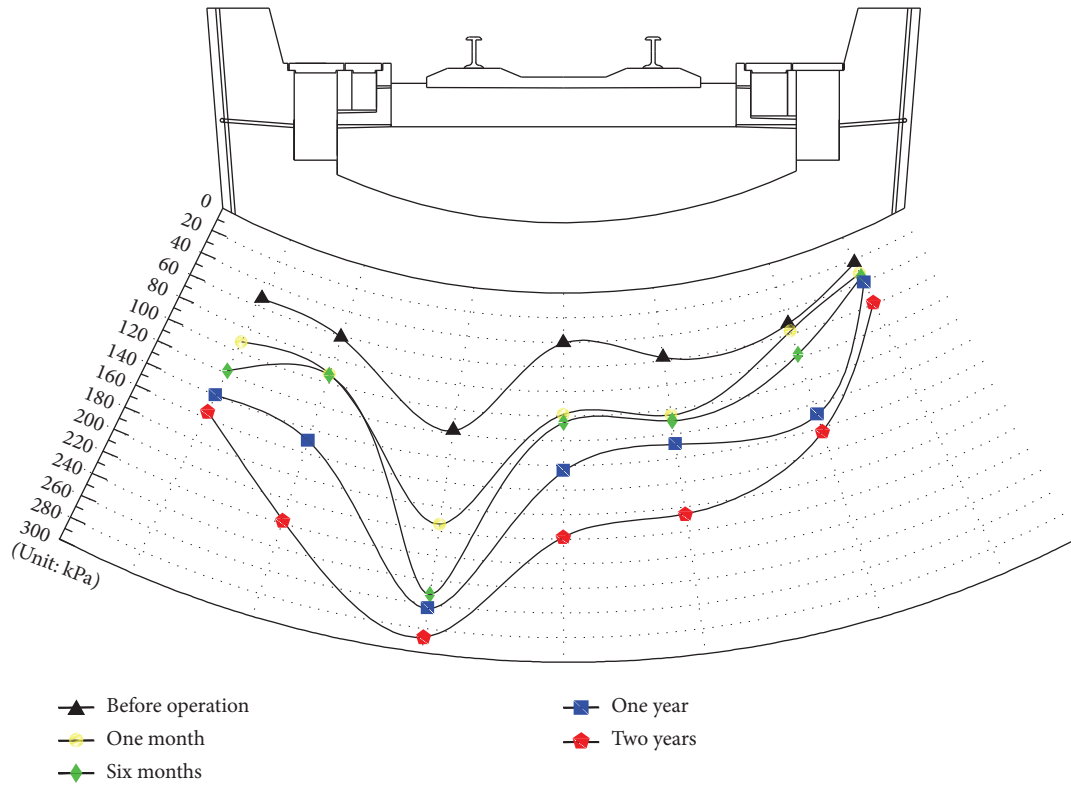


FIGURE 8: Water pressure change diagram of surrounding rock at the bottom.

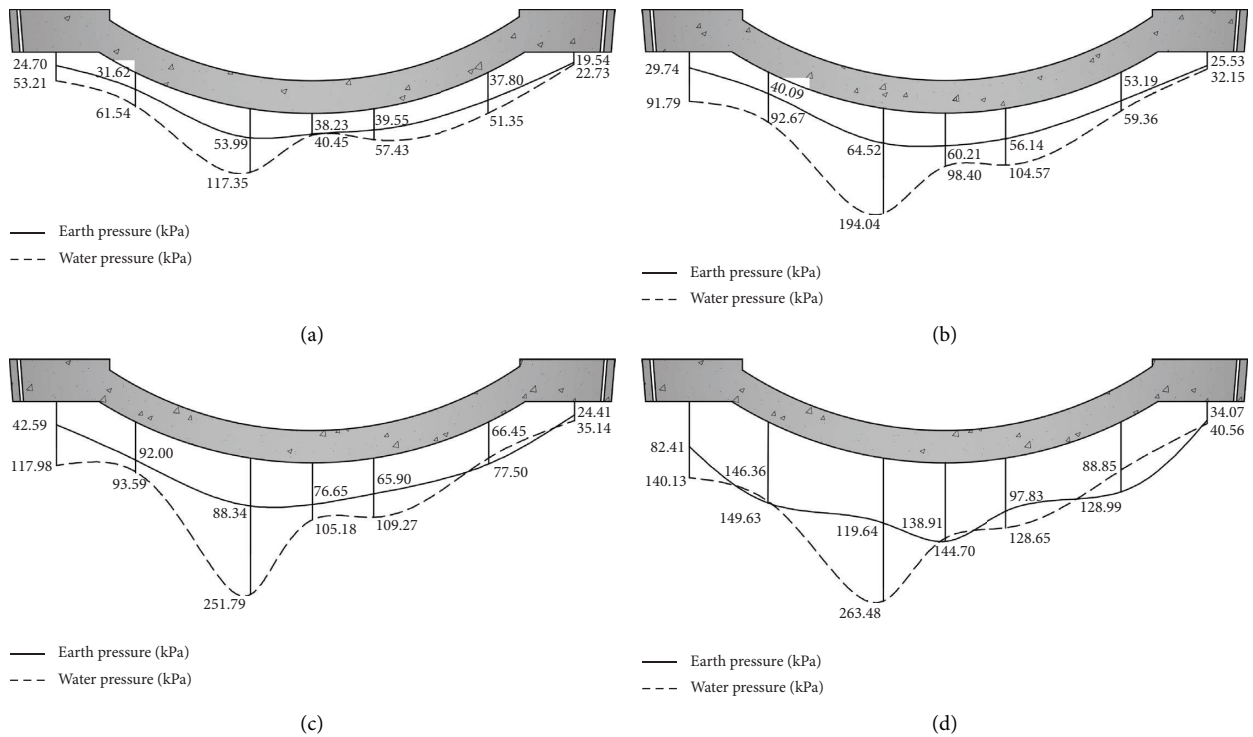


FIGURE 9: Continued.

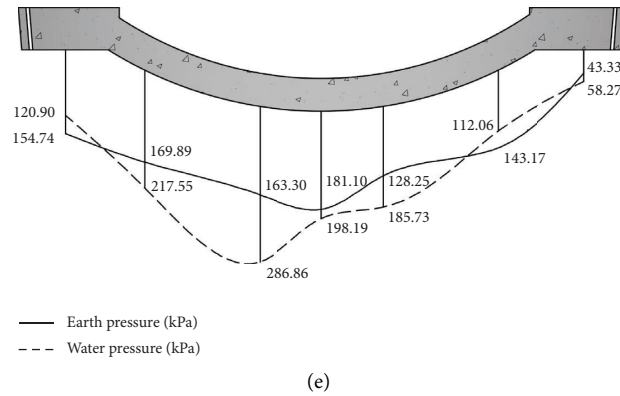


FIGURE 9: Relationship between the earth and water pressure of the basement rock: (a) before operation; (b) one month; (c) six months; (d) one year; (e) two years.

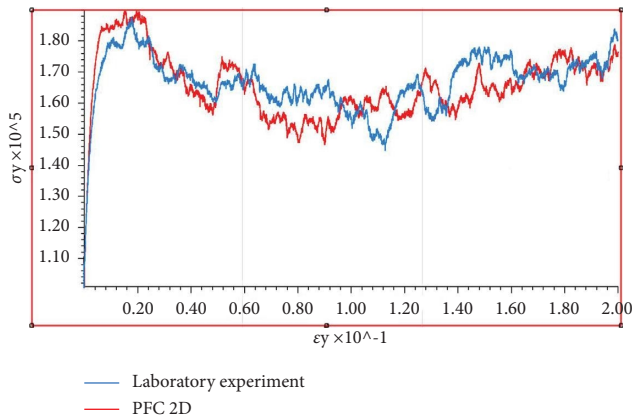


FIGURE 10: Comparison of stress-strain between laboratory experiment and discrete element simulation.

element simulation is consistent and the fit is good, the error is small, and the calibration standard is met.

4.2. Establishment of the Discrete Element Model

4.2.1. Calibration of Surrounding Rock Parameters. According to Article 4.3.3 of the code for the design of railway tunnels [12], the PFC2D discrete element model is set up by calibration according to the actual condition of the surrounding rocks of the Taihangshan Mountain Tunnel. The model is composed of four sides. The sample loading is simulated by controlling the speed of the top and bottom surfaces, and the surrounding rock pressure is simulated on the left and right surfaces. When loading on the top and bottom, the left and right sides move along to ensure that the confining pressure within the scope of the model remains in equilibrium.

4.2.2. Establishment of Surrounding Rock Model. Conduct comprehensive analysis according to the measured monitoring results, the cavity of the basement rock mainly appears in the center of the railway, and this principally results from the deterioration of the surrounding rock

caused by the action of train load and groundwater erosion. Due to the computational efficiency of PFC2D particle flow software, the size of the model should be controlled appropriately; therefore, the PFC2D discrete element model is simplified to some extent, as shown in Figure 11.

In PFC2D, the material is composed of the interaction of the rigid spherical contact. The particle material of the surrounding rock model in this study uses the linear model to simulate the granular Class V surrounding rock. The model is splitted into the following two parts: the surrounding rock and the inverted arch. The loading of the sample is simulated by controlling the velocity of the inverted arch wall. To facilitate calculation, this model idealized irregular surrounding rock particles into regular round particles and finally formed 3827 particles into a 100 cm × 100 cm model. The mesoscopic correlation parameters of the surrounding rock model are shown in Table 2.

4.2.3. Hydrodynamic Model of the Tunnel Bottom. The scouring effect of dynamic water on base rock caused by heavy-haul train load is the main cause of the cavity at the bottom of the tunnel. Therefore, the water pressure magnitude is the key to ensuring the objective accuracy of the simulation. The hydrodynamic pressure value calculated is determined based on the data of field monitoring of the Taihangshan Mountain Tunnel in the early stage. Based on the field-measured inverted arch water pressure time-history curve, the pore water pressure at each monitoring position increases with time and the value ranges from 0 to 300 kPa. Therefore, the water flow range is 0–18 m/s. The particle flow model is shown in Figure 12.

In Figure 12, the red surrounding the model is an impermeable and fixed boundary. Some particles were deleted near the track position of the inverted arch bottom to simulate the initial defect of the basement rock, and a velocity-changing boundary was applied to simulate the flow of high-pressure pore water. Tian et al. [17], in the high-pressure flow field, the pipe network model is generally used to simulate fluid-solid coupling. After the formation of the surrounding rock model is stable, a water particle is

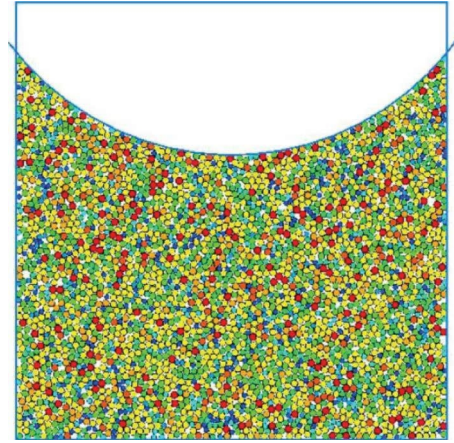


FIGURE 11: Particle flow model of surrounding rock.

TABLE 2: Microparameters of surrounding rock model.

Particle size ratio (R_{\max}/R_{\min})	Density ρ ($\text{g}\cdot\text{cm}^{-3}$)	Friction coefficient (μ)	Contact modulus of particles (E_c/GPa)	Stiffness ratio of particle (k_n/k_s)
1.5	2.7	0.5	0.1	2

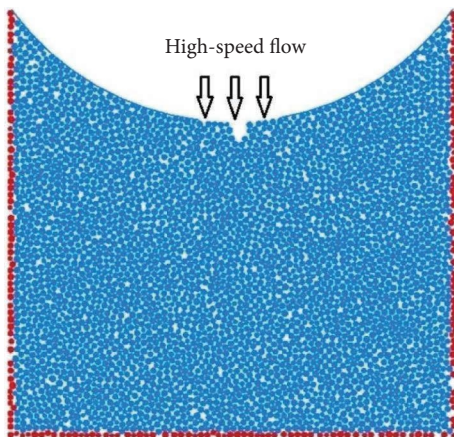


FIGURE 12: Implication diagram of dynamic flow in the granular flow model.

generated at the contact point of the surrounding rock particles, and the water particles are connected to form a pipe channel. Finally, an entire pipe network is formed. In the calculation process, the pressure of water particles will continue to update and act on the surrounding rock particles. The model of the pipe network is shown in Figure 13, and the microscopic parameters of the fluid grid are shown in Table 3.

4.2.4. Simulation of Train Dynamic Load. In this simulation, the load is directly applied to the ball particles to increase the speed or concentration through the ball interaction force transmission. In order to simplify the arithmetic based on the measured acceleration curve. The velocity curve corresponds to the sinusoidal velocity applied to the permeable boundary of the upper particle surface of the model:

$$V(t) = V_0 \cdot \sin(2\pi ft), \quad (1)$$

where V_0 is the half peak velocity, f is frequency, and t is the excitation time.

4.2.5. Calculation Conditions. To study the formation process and the degradation degree of the basement surrounding rock cavity in a water-rich environment, four working conditions are set according to the operation time to simulate the long-term scouring action of groundwater on the basement rock. The high-speed flow increases gradually at 2 m/s. The calculation conditions are shown in Table 4.

4.3. Discrete Element Calculation Results

4.3.1. Law of Surrounding Rock Degradation. With the increase of hydrodynamic pressure and operation time, the deterioration of the basement rock is gradually developed, as shown in Figure 14.

As shown in Figure 14(a), before the operation of the tunnel in a water-rich environment, the initial damaged position of the basement surrounding rock generates hydrostatic pressure owing to water accumulation, and the surrounding rock is less eroded by water. One month after the use of the tunnel, the static water at the initial damage point of the basement rock under train loads is subject to dynamic flow, which causes a scouring effect on the surrounding rock and further aggravates the deterioration of the basement rock.

As shown in Figure 14(b), as the operating time increases, the cavity of the surrounding rock further expands, and cracks appear in the adjacent position. After six months of operation, the cracks in the surrounding rock of the

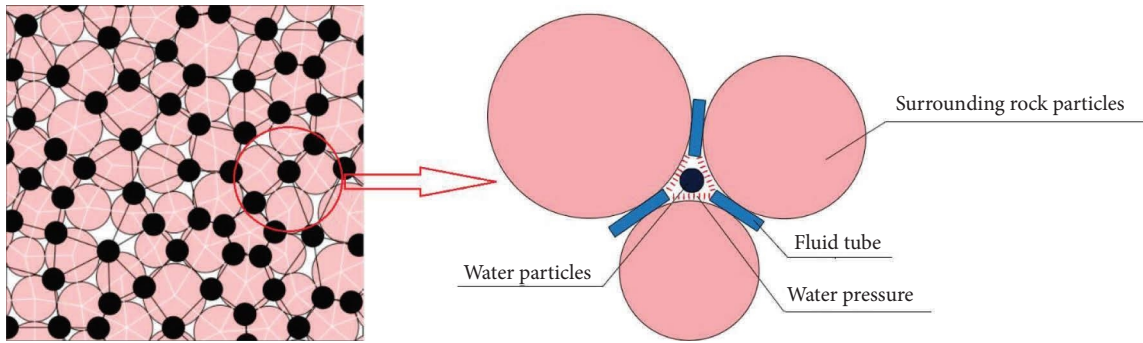


FIGURE 13: Flow tube network model.

TABLE 3: Microparameters of the fluid grid.

Fluid density (kg/m ³)	Flow velocity (m/s)	Viscosity coefficient (Pa·s)	Permeability coefficient (cm/s)
1000	0~14	1.0×10^{-3}	4

TABLE 4: Calculation conditions of a discrete element.

Working condition number	Surrounding rock classification	Train axle (kN)	High-speed flow (m/s)	Service time
1	V	300	2 m/s~14 m/s	One month
2			2 m/s~15 m/s	Six months
3			2 m/s~16 m/s	Two years
4			2 m/s~17 m/s	Four years

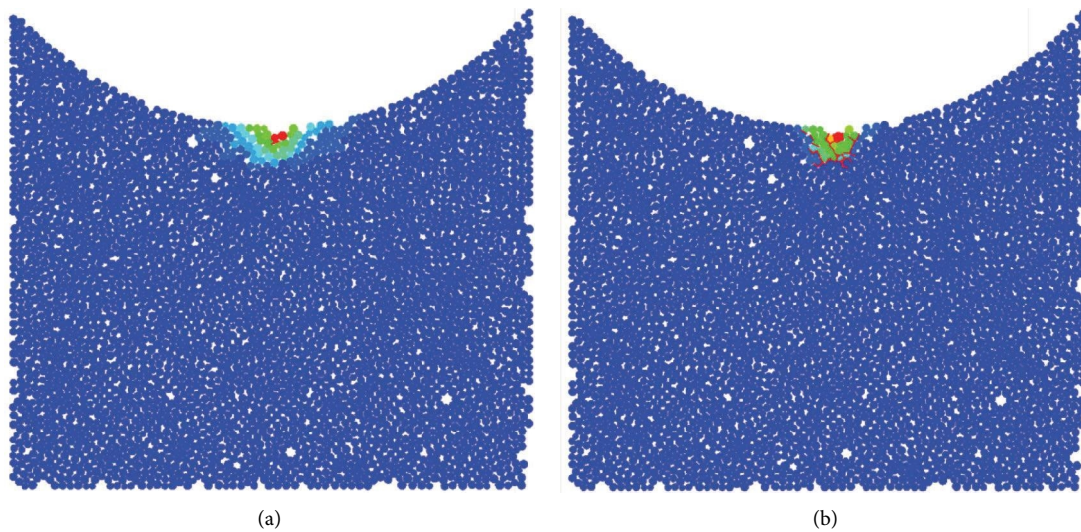


FIGURE 14: Continued.

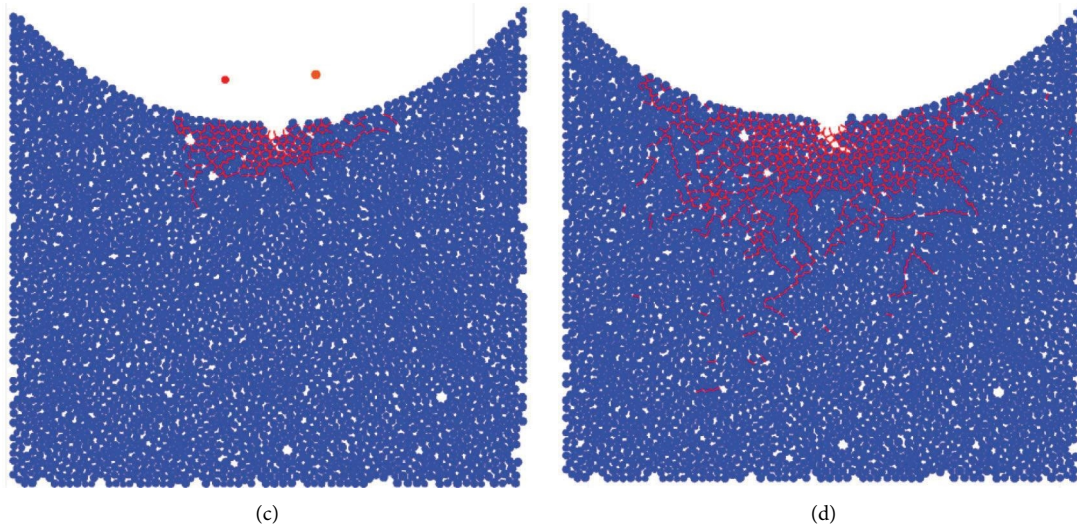


FIGURE 14: Development law of surrounding rock cracks: (a) one month; (b) six months; (c) two years; (d) four years.

TABLE 5: Development table of cavity deterioration of base rock.

Operation days (day)	Number of particle loss in the surrounding rock	Fracture number	Average width (cm)	Average depth (cm)
30	3	1	—	—
180	10	34	10	6
730	21	242	38	10
1460	35	2150	89	40

basement are interconnected and radial, and the number of cracks increases to 34 during the operation, with an average width of approximately 10 cm and an average depth of approximately 6 cm.

As shown in Figure 14(c), after two years of operation, the range of the surrounding rock cracks is expanded and some surrounding rock particles are gradually lost. The development of cracks takes the basement surrounding rock cavity as the center and presents a crescent distribution. The number of cracks increased from 34 in half a year of operation to 242, with an increase of approximately 612%, with an average width of approximately 38 cm and an average depth of approximately 10 cm.

As shown in Figure 14(d), after four years of operation, the cracks penetrated the entire basement surrounding rock, providing numerous water flow channels for the loss of rock particles. The number of cracks increased from 242 in two years of operation to 2150, an increase of about 788%. The particle loss of rock changes from 3 to 35. The average width of cracks was approximately 89 cm, and the average depth was approximately 40 cm. According to the development law of cracks in five years of operation, the results are shown in Table 5.

From Table 5, as the operating time increases, the number and range of cracks in the basement rock continue to increase, and the initial damage at the center spreads to the adjacent position to cause the continuous cavity of the

surrounding rock. In addition, the development of cracks provides many water channels, causing the surrounding rock particles to continue to drain and form cavities.

4.3.2. Contact Chain of Rock Particles. From Figure 14, it can be seen that when the particles are eroded by the water flow, the connection between the particles fails, and cracks are generated, but the cracks and contact chains are dynamically reflected in the monitoring process in real time. The particles that originally generated cracks can regenerate the contact phenomenon under the action of the water flow, which leads to the difference between the cracks and the contact chain.

The contact chain between particles can further determine the deterioration degree and the integrity of the basement rock. The contact of surrounding rock particles in the characteristic stage is shown in Figure 15.

According to Figure 15, the contact chain between the surrounding rock particles is relatively weak owing to the poor cementation of Class V surrounding rock. As shown in Figure 15(a), the contact chain of rock particles is “strong above and weak below.” This is because the dynamic water flow caused by the train load penetrates the rock particles through the initial damage of the basement rock, resulting in the squeezing pressure between the rock particles, thus showing the phenomenon of enhanced contact force.

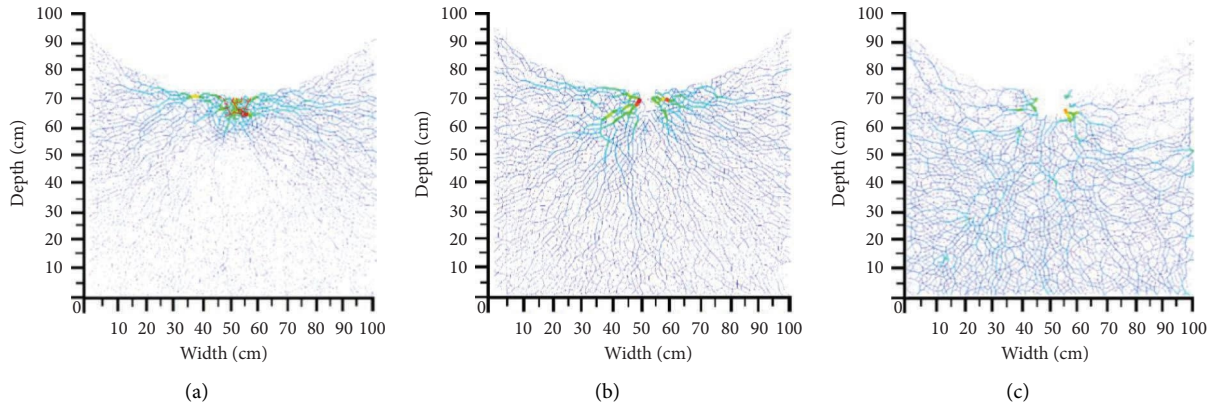


FIGURE 15: Contact chain distribution of base rock particles: (a) one month of operation; (b) two years of operation; (c) four years of operation.

According to Figure 15(b), as the operating time increases and under the combined action of train load and dynamic water, the surrounding rock particles are partially lost, and the contact chain leads to local fracture. The contact chain distribution of rock particles is uniform. However, the contact chain is still strong owing to the particle extrusion caused by water scouring the cavity.

According to Figure 15(c), the distribution of the rock contact chain reached an equilibrium state under long-term operation conditions, and the distribution law of the contact chain is generally characterized by “upper weak and lower strong.” This is because the contact between the surface surrounding rock particles is damaged or destroyed under long-term train load and hydrodynamic scouring, and the particles of the lower surrounding rock are gradually balanced owing to gravity.

The particle loss results and particle contact chain distribution characteristics of PFC surrounding rock are comprehensively analyzed. For the heavy-haul railway tunnel under the condition of rich water, under the dynamic load of 300 kN axle load, the extent of damaged contact part between the invert structure and the basement rock is significantly increased after two years of operation, and the rock mass integrity is significantly reduced. The increase in the water flow channel provides conditions for the further loss of the rock particles. At this time, the effect of surrounding rock cavity deterioration on the damage to the bottom structure also increases. Combined with the measured data of water-earth pressures, the degradation process of the basement surrounding rock is divided into three characteristic stages: the first stage is the early stage of operation, the integrity of the basement surrounding rock is good, and the arch structure is dense. Some gaps exist owing to construction or geological conditions. The second stage is the local cavity of the basement surrounding rock. With time, the groundwater in the cavity position continuously scours the basement surrounding rock under a dynamic action to form a local cavity and develops over time, and the integrity of the basement surrounding rock is influenced. The third stage is cavity penetration. Here, the incomplete contact between the surrounding rock of the basement and

the invert structure continues to develop, and the local cavity penetration caused the stress of the bottom structure of the tunnel to become unbalanced and easy to form the corresponding diseases.

5. Damage Analysis of the Bottom Structure of the Double-Track Heavy-Haul Railway Tunnel

5.1. Fatigue Damage Calculation Model. The calculation model of double line heavy-haul railway tunnel is established by using the finite element calculation software Workbench. The model is established by a three-dimensional solid element Solid185. The rock width on both sides of the tunnel is 5 times the hole diameter and it below the tunnel is 4 times (eliminating the border effect). Liu et al. [18], Peng et al. [19], and Yao and Hu [20, 21], the concrete structure is simulated by the elastic model and the rock is simulated by the elastic-plastic model. There is setting of artificial viscoelastic boundary at the bottom and both sides of the calculation model. The model is shown in Figure 16.

The calculation parameters of surrounding rock and structural parameters in the stratum structure model are selected as shown in Tables 6 and 7.

5.2. Train Dynamic Load Simulation Method. The dynamic load time-history curve (Figure 17) of 300 kN axle load measured in the field of the Fuyingzi Tunnel is imported into ANSYS Workbench simulation software as the initial dynamic condition in fatigue damage analysis, which is applied to the track position of the ballast of the heavy-haul tunnel. The equivalent dynamic load of 17 t axle load is applied on the right conventional railway line according to the equal ratio reduction of measured data.

Presently, the annual traffic volume of heavy-haul railways in China has increased. Meanwhile, the yearly traffic volume of Daqin Railway is obviously higher than 40 million tons [22]. Therefore, the annual cumulative loading number is set to 1.5 million times to simulate the annual traffic of the

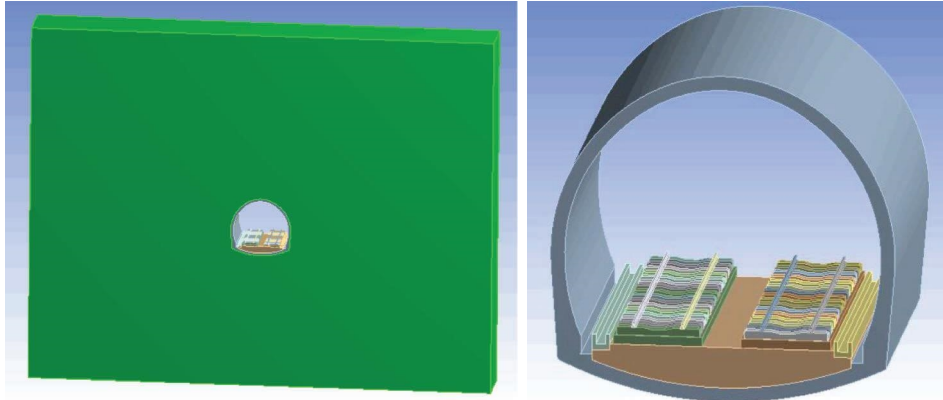


FIGURE 16: Fatigue damage analysis based on finite element method.

TABLE 6: Structural physical mechanics parameters.

Structure	Material	Element	Elastic modulus (GPa)	Poisson ratio	Gravity (kN/m ³)
Secondary lining	C30	SOLID45	31	0.20	23
Track bed	C40	SOLID45	33.5	0.20	25
Inverting fill	C20	SOLID45	28.5	0.20	23
Inverted arch	C30	SOLID45	31	0.20	23
Pillow	—	SOLID45	52.4	0.30	25

TABLE 7: Physical and mechanical parameters of surrounding rock.

Surrounding rock grade	Element	Elastic modulus (GPa)	Poisson ratio	Gravity (kN/m ³)	Cohesion (MPa)	Friction angle (°)
III	SOLID45	13	0.27	24	1.1	65
IV	SOLID45	3.6	0.33	21.5	0.45	55
V	SOLID45	1.5	0.4	18.5	0.125	45

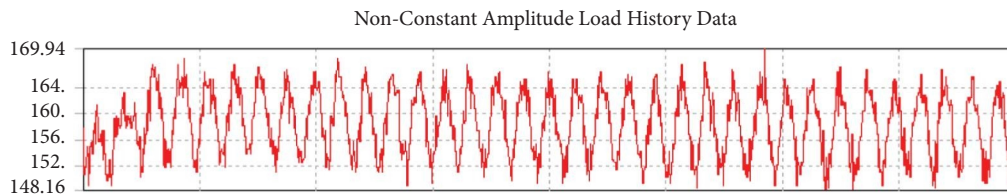


FIGURE 17: Power supply initial conditions of Workbench simulation software.

Fuyingzi tunnel of 45 million tons and cumulative calculation of 100 years.

5.3. Analysis Method of Fatigue Damage. Miner proposed the linear fatigue cumulative damage theory; according to the theory, the fatigue life of a heavy-haul railway tunnel is analyzed according to the S-N curve, which is a widely used damage theory [22]. When the train goes through the tunnel, the tunnel structure undergoes a cycle of variable amplitude stress. Based on Miner's linear fatigue cumulative damage,

the structure's fatigue damage that resulted from a single train is shown in the equation as follows:

$$D' = \sum_i^n \frac{n_i}{N_i}, \quad (2)$$

where D' is the structure's fatigue damage that resulted from a single train, n_i is the number of cycles of stress amplitude $\Delta\sigma_i$, and N_i is the cycle number of concrete subjected to fatigue failure under the action of stress amplitude $\Delta\sigma_i$.

The S-N curve characterizes the relationship between the loading cycles number N (fatigue life) that can be withstood by the material before fatigue damage and the stress amplitude $\Delta\sigma$ of the component, and the $\Delta\sigma$ is generally expressed by a power function and an exponential. In this study, the concepts of homotactic fatigue life and stress level are adopted by Cao et al. [23]. Combined with the three-parameter Fardis–Chen model and the modified Aas–Jakobson equation, the multiaxial stress S-N curve of concrete is shown in the following equation:

$$S_{\max} = 1.0170 - 0.0608 \log N, \quad (3)$$

where S denotes the structure's stress level, N denotes the fatigue life, and the parameter also reflects the number of cyclic loadings during fatigue aging.

The basement structure's damage in Workbench is evaluated by damage value. The damage value is the specific value of the design service life to the available life of a structure, as shown in equation (4). So, when the damage value attains 1, the concrete here has fractured and failed.

$$\text{Damage} = \frac{\text{Life}_{\text{Design}}}{\text{Life}_{\text{Available}}}, \quad (4)$$

where damage represents the structure's damage value, $\text{Life}_{\text{Design}}$ indicates the design life of the tunnel structure, which is selected according to 100 years, and $\text{Life}_{\text{Available}}$ represents the utilizable life of the tunnel structure.

5.4. The Analysis Results of Fatigue Damage

5.4.1. Fatigue Damage Feature of the Basement Structure.

The damage distribution of the bottom structure under 30 t axial load in the initial state of V surrounding rock is shown in Figure 18.

As shown in Figure 18, the maximum damage value is formed by the boundary effect of the longitudinal end. However, there is a certain particularity in this position. The end of the model is not analyzed using this method. Based on fatigue damage analysis, the heavy-haul railway tunnel's damage is mainly focused on the bottom, while the damage accumulation of the lining structure is weak. In addition, the damage extent of the heavy-haul railway in the bottom structure is more serious than that of common passenger and freight railways, and the structure's damage is mainly focused on the track vertical position of each structural layer, which indicates that the damage of the tunnel's basement structure is basically developed from the orbit position. The damage values and time of the bottom structure track bed, filling, and invert structure corresponding to three characteristic stages of Class V surrounding rock (denser, local cavity, and cavity connection) are listed in Table 8.

As shown in Table 8, the three states of the surrounding rock have different degrees of influence on the distribution of fatigue damage of the basement structure. The specific analysis is as follows:

- (1) When the completeness of the surrounding rock is appropriate in the first stage, the fatigue lifetime of

the basement structure of the tunnel increases from above to below; however, the damage extent raises at the same time. The fatigue life of the side track bed of heavy-haul railway under 300 kN axle load is 76 years, which is 14.44% lower compared with the ordinary railways. The filling structure's fatigue lifetime of the heavy-haul railway is 90 years, which is 14.15% lower compared with ordinary railways. The invert structure's fatigue lifetime of the heavy-haul railway is almost 119 years, 6.30% lower than the ordinary railway. The impact of train dynamic load on the fatigue damage of the substructure weakens stage by stage from above to below, and the damage is expanded from above to below.

- (2) When local cavities appear in the surrounding rock under the second working condition, the fatigue lifetime of all parts of the base structure decreases. The fatigue lifetime of the track bed structure on the heavy-haul load and conventional railway line sides decreased to 67 and 80 years, which were 11.8% and 10.1% lower than those in the first stage, respectively. The filling structure's fatigue lifetime on the sides of the heavy-haul line and the conventional railway line decreased to 75 and 91 years, which were 16.7 and 14.2% compared with the first stage, respectively. The invert structure's fatigue lifetime on the heavy load and conventional railway line sides decreased to 79 and 98 years, corresponding to a decrease of 33.6% and 22.8% compared with the first stage, respectively. The cumulative damage of backfill and inverted arch structure increases significantly with the debasing of the surrounding rock state. The closer the distance to the deterioration position of the surrounding rock, the faster the decrease in structural life.
- (3) When the surrounding rock is in the third stage cavity connection, the fatigue lifetime of each part of the bottom structure decreases significantly. Among them, the fatigue lifetime of the invert structure decreased the most, and the invert structure's fatigue lifetime on the heavy-haul and conventional railway line sides decreased to 51 and 90 years, which were 57.1% and 29.1% lower than those in the first stage, respectively. The joint action of the surrounding rock degradation and heavy-haul train dynamic load not only enabled the rapid development of the structural damage of the heavy-haul line side but also indirectly aggravated the structural damage of the conventional railway line side and significantly reduced the overall stress safety of the bottom structure.

To further analyze the development law of fatigue damage of substructure during operation, the development law of the basement structure's fatigue damage in the 5th, 20th, and 80th years under the three characteristic stages of Class V surrounding rock is shown in Figures 19 and 20.

From Figures 19–21, the damage distribution of the bottom structure corresponding to the three characteristic stages of the surrounding rock increases from above to below

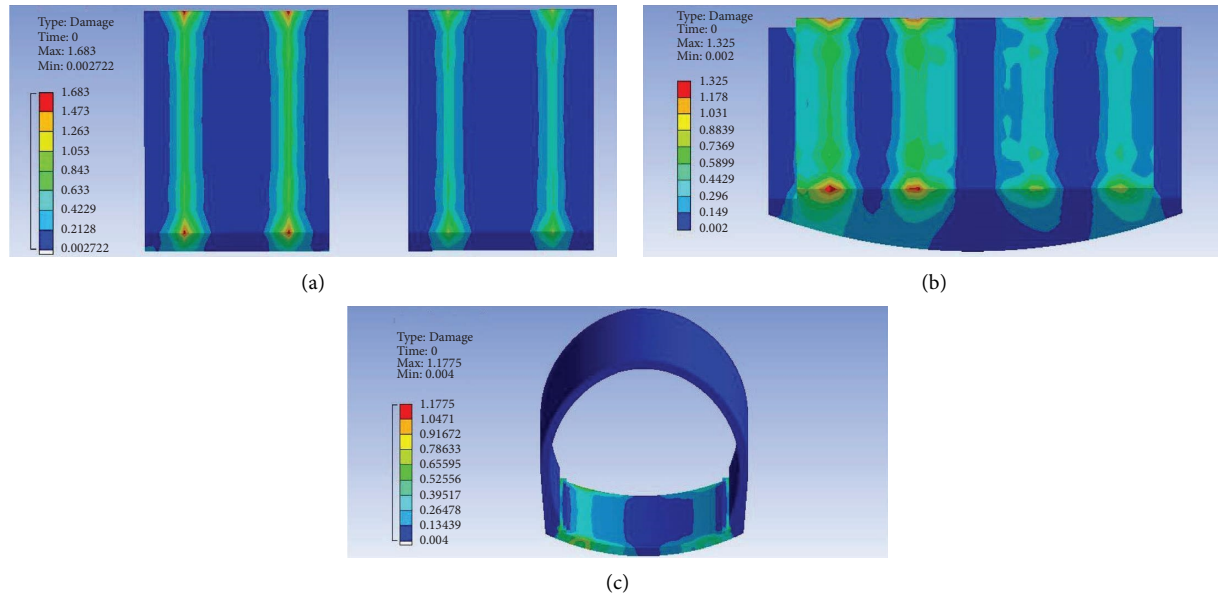


FIGURE 18: V damage distribution map of the bottom structure of the surrounding rock: (a) ballast bed structure; (b) filling structure; (c) invert structure.

and the damage degree of the heavy-haul line is significantly higher compared with the conventional railway line side. In addition, with a decrease in the surrounding rock integrity and the development of a local cavity, the fatigue failure of the basement structure aggravated, as follows:

The bottom structure failure corresponding to the three stages of surrounding rock in the fifth year of operation is the first position of the side ballast structure of the heavy-haul line. The worse the integrity of the surrounding rock, the faster the development rate of structural damage and the greater the degree and scope of damage simultaneously. When the surrounding rock is disconnected and penetrated, the operation of heavy-haul lines is only five years, and the damage to the side and bottom structures have a semiconnected trend.

In the 20th year of operation, the bottom structural damage of the three surrounding rock stages continued to develop, and the worse the state of the surrounding rock, the more intense the corresponding bottom structural damage. Among them, when the surrounding rock is a cavity and connected, the inverted arch failure of the substrate structure develops reversely from the cavity position of the surrounding rock under the dynamic action.

The damage characteristics of the bottom structure corresponding to the three stages of the surrounding rock show significant differences in the 80th year. When the surrounding rock is in the stage of a good fit, the damage to the bottom structure is mainly concentrated in the ballast bed structure at one side of the heavy-haul line indicating that when the surrounding rock integrity is

good, axle load rolling is the main cause of fatigue damage development of bottom structures. When a local cavity occurs in the surrounding rock, the failure of the bottom structure is mainly focused on the connection between the orbital position and the local cavity of the surrounding rock, and thus develops to the surrounding. When the basement rock is a cavity and penetrated, the bottom structural damage develops reversely from the cavity position, which significantly increases the damage degree and scope, and influences the structural stress safety at the bottom of the left groove. At this time, the fatigue lifetime of the structure on the connection between the track and the cavity positions is lower than the 100-year design requirement, and the damage to the ballast bed structure is particularly serious.

Based on comprehensive analysis and judgement, the deterioration of the bedrock and the dynamic action of heavy-haul trains aggravate the bottom structural damage, and the rolling enables the development of the bottom structure damage from top to bottom to track the position of the track bed. The effect of basement rock degradation on the failure development of the bottom construction is reversed; the invert structure develops from bottom to top from the degradation position of the basement rock. Finally, the bottom structure's damage is mainly concentrated in the connection between the degradation position of the surrounding rock and the track. The cavity and deterioration of the bedrock are extremely unfavorable to the stress safety of the bottom structure. Due to the comprehensive effect of train dynamic action, the fatigue life of the bottom structure is difficult to meet the design requirements.

TABLE 8: V surrounding rock fatigue damage calculation results of bottom structure in three characteristic stages.

State of surrounding rock	Structure part	Maximum damage value		Cumulative loading times (ten thousand times)			Fatigue lifetime (year)		Location of damage	
		Heavy-haul railway	Conventional railway	Heavy-haul railway	Conventional railway	Conventional railway	Heavy-haul railway	Conventional railway	Heavy-haul railway	Conventional railway
Phase I: denser	Track bed	1.315	1.123	1.13×10^4	1.33×10^4	76	89	Below the track		
	Filling	1.112	0.944	1.36×10^4	1.59×10^4	90	106	Below the track		
	Inverted arch	0.840	0.787	1.79×10^4	1.91×10^4	119	127	Area below the line		
Phase II: local cavity	Track bed	1.493	1.250	1.01×10^4	1.20×10^4	67	80	Below the track		
	Filling	1.333	1.099	1.13×10^4	1.37×10^4	75	91	Below the track		
	Inverted arch	1.266	1.020	1.19×10^4	1.47×10^4	79	98	The area below the line		
Phase III: cavity connection	Track bed	2.381	1.282	0.63×10^4	1.17×10^4	42	78	Below the track		
	Filling	1.724	1.136	0.87×10^4	1.32×10^4	58	88	Below the track		
	Inverted arch	1.961	1.111	0.77×10^4	1.35×10^4	51	90	The area below the line		

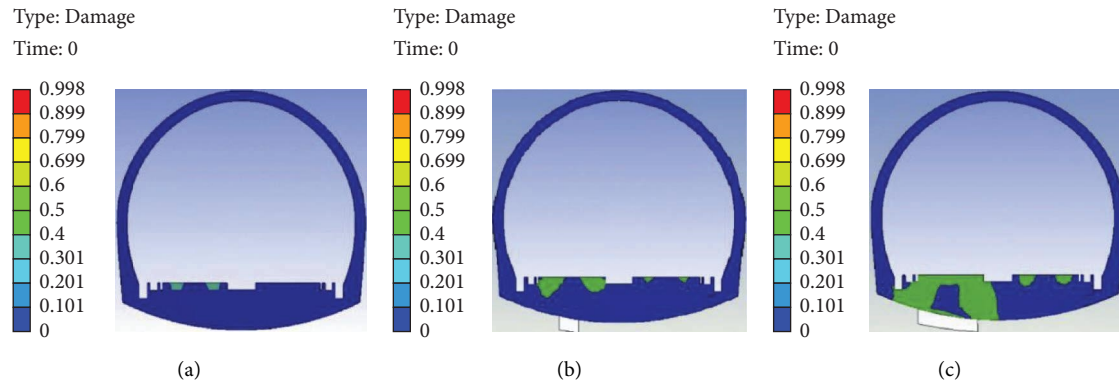


FIGURE 19: Distribution characteristics of substructure damage in three stages of surrounding rock in the fifth year of operation: (a) denser; (b) local cavity; (c) cavity connection.

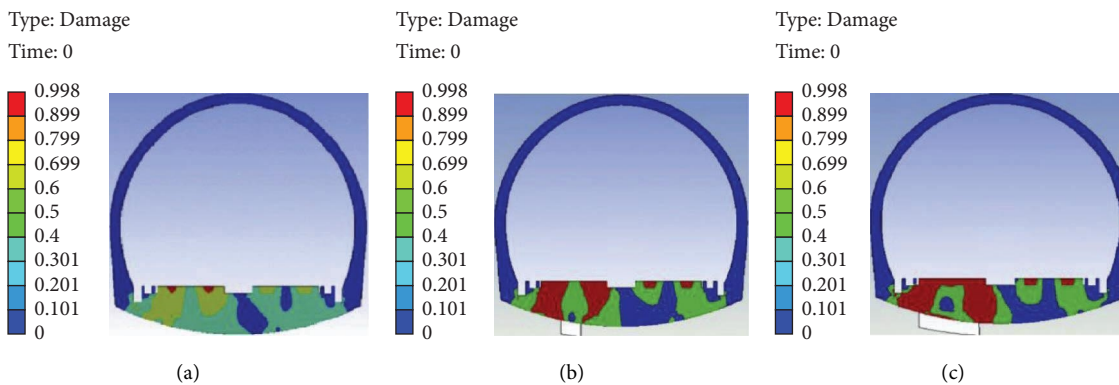


FIGURE 20: Distribution characteristics of substructure damage in three stages of surrounding rock in the 80th year of operation: (a) denser; (b) local cavity; (c) cavity connection.

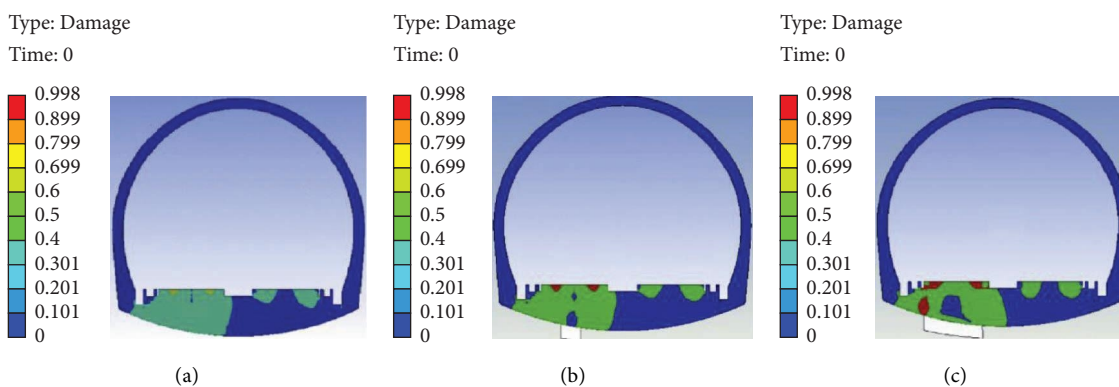


FIGURE 21: Distribution characteristics of substructure damage in three stages of surrounding rock in the 20th year of operation: (a) denser; (b) local cavity; (c) cavity connection.

6. Conclusions

According to the measured water-earth pressures data of the base rock of the Taihangshan Mountain Tunnel obtained from the previous long-term monitoring, and based on the

analysis of discrete element software, the law of cavity deterioration in bedrock is clarified in this study, which is used as the research basis for the structural damage analysis of the bottom of the double-track heavy-haul railway tunnel. The influence of various degrees of the basement rock

deterioration on the structural damage of the bottom of the tunnel is analyzed, and the following conclusions are obtained:

- (i) Affected by long-term heavy axle load rolling of heavy-haul trains, the water-earth pressures on the bedrock surface increase continuously, and the increase at the left measuring point is significantly higher compared with the right. Based on the measured results, when the heavy-haul railway tunnel was in operation, the initial defects of the basement surrounding rock formed cavities and caused groundwater accumulation, and finally formed a high hydrodynamic pressure, which aggravated the long-term effect of earth pressure at adjacent locations.
- (ii) Upon completion of the construction of the bottom structure, owing to objective defects such as virtual ballast at the bottom, conditions were provided for groundwater accumulation and water channel development. According to the discrete element simulation analysis, when subjected to the long-term dynamic action of the train, the surrounding rock will collapse from the initial damage location and particle loss to reduce the integrity, thus influencing the water-earth pressure distribution of the basement surrounding rock. According to the operation time and surrounding rock degradation degree, the degradation process of the basement surrounding rock cavity is divided into three characteristic stages: good surrounding rock fit, local cavity, and cavity connection.
- (iii) For double-track heavy-haul railway tunnels, when the integrity of surrounding rock was good, structural damage at the tunnel bottom was principally induced by the axle load, and the influence on the range and life of structural fatigue damage was gradually weakened from above to below. Accompanied by the deterioration of the basement rock, the fatigue lifetime of each part of the bottom structure of the tunnel was significantly reduced under the effect of train dynamic action, with a maximum decrease of 57.1%. Meanwhile, the conventional railway line side was indirectly influenced as well, which reduced the overall stress stability of the bottom structure.
- (iv) The influence of basement rock degradation on tunnel bottom structure damage gradually weakened from above to below. When subjected to the action of the water and train dynamic load, the bottom structural damage was down from the track position of the track bed, and the empty position of the inverted arch surrounding rock was up, developed synchronously, and finally focused on the connection between the track and the deterioration position of the surrounding rock. The larger the deterioration scale of the surrounding rock, the wider the damage range of the bottom structure, the

faster the damage developed, and the more severer the damage; the actual service life of the bottom structure rarely met the design requirements.

Data Availability

The datasets used or analyzed during the current study are available from the corresponding author upon reasonable request.

Conflicts of Interest

The authors declared that they have no conflicts of interest.

Acknowledgments

This study was supported by the National Natural Science Foundation of China (5108098 and 51908387), the China Postdoctoral Science Foundation funded project (2022M720594), the Chongqing Natural Science Foundation (General Project) (CSTB2022NSCQ-MSX0518), the Open-End Fund of Key Laboratory of New Technology for Construction of Cities in Mountain Area (LNTCCMA-20210108), the Chongqing Municipal Construction Investment (Group) Co., Ltd. Joint Technical Issues (CQCT-JSA-GC-2021-0138), the Chongqing Natural Science Fund General Project (cstc2020jcyj-msxmX0904), the Chongqing Talents: Exceptional Young Talents Project (cstc2021ycjh-bgzxm0246), the China Postdoctoral Science Foundation-General Project (2021M693739), the Chongqing Outstanding Youth Science Fund Project (2022NSCQ-JQX1224), and the Special Funding for Postdoctoral Research Projects in Chongqing (2021XM2019).

References

- [1] H. Li, "Comprehensive description of heavy haul railways abroad," *Journal of Railway Engineering Society*, vol. 17, no. 4, pp. 32–34, 2000.
- [2] Z. Q. Li, *Research on the dynamic characteristics and design method of heavy haul railway tunnel structure*, PhD Thesis, SouthwestJiaotong University, Chengdu, China, 2018.
- [3] C. Shi, M. Lei, L. Peng, W. Yang, and Z. Ding, "In-situ monitoring and analysis of mechanical characteristics and deformation of bottom structure of tunnels," *Chinese Journal of Geotechnical Engineering*, vol. 34, no. 5, pp. 879–884, 2012.
- [4] W. Zou, M. Zhang, Y. Liu, and W. Ma, "Stress distribution and dynamic response of base structure for heavy haul railway tunnel under 30 t axle load," *China Railway Science*, vol. 37, no. 5, pp. 50–56, 2016.
- [5] Y. Niu, *The Heavy Haul Railway Tunnel Diseases Mechanism and Remediation Technology Research*, China Academy of Railway Sciences, Beijing, China, 2013.
- [6] Q. Su, H. Bai, J. Huang, L. I. Xing, and W. Zhang, "In-situ tests on long-term dynamic characteristics of low embankment on rigid foundation," *China Civil Engineering Journal*, vol. 44, no. 1, pp. 147–151, 2011.
- [7] S. K. Mandal and M. M. Singh, "Evaluating extent and causes of overbreak in tunnels," *Tunnelling and Underground Space Technology*, vol. 24, no. 1, pp. 22–36, 2009.
- [8] S. Jeon, J. Kim, Y. Seo, and C. Hong, "Effect of a fault and weak plane on the stability of a tunnel in rock-a scaled model test

- and numerical analysis,” *International Journal of Rock Mechanics and Mining Sciences*, vol. 41, no. 3, pp. 658–663, 2004.
- [9] W. L. Hamilton, H. A. Sorebo, W. G. Reeves et al., *Absorbierender Artikel Mit Faserbündeln Und Rieselfhigen Partikeln Absorbent Articles with Fiber Bundle and Free-Flowing Particles*, CN00,806,297.8, Kimberley Clark Global Co., Ltd., 2007.
- [10] L. Ning, L. Peng, C. Shi, and W. Yan, “Analysis of the influence of basis conditions on the dynamic response of a bottom structure of a heavy haul railway tunnel and its service life,” *Modern Tunnelling Technology*, vol. 53, no. 5, pp. 114–122, 2016.
- [11] L. Gao, J. Luo, and L. Wang, “Analysis of vibration characteristics and life prediction of inverted arch under base cavity,” *Journal of Civil Engineering*, vol. 53, no. 1, pp. 348–354, 2020.
- [12] TB 10003-2016, *Code for Design on Tunnel of Railway*, Railway Publishing House, Beijing, China, 2005.
- [13] F. Khamitov, N. H. Minh, and Y. Zhao, “Coupled CFD–DEM numerical modelling of perforation damage and sand production in weak sandstone formation,” *Geomechanics for Energy and the Environment*, vol. 28, Article ID 100255, 2021.
- [14] D. X. Liang, N. Zhang, H. Y. Liu, D. Fukuda, and H. Y. Rong, “Hybrid finitediscrete element simulator based on GPGPU-parallelized computation for modelling crack initiation and coalescence in sandy mudstone with prefabricated cross-flaws under uniaxial compression,” *Engineering Fracture Mechanics*, vol. 247, Article ID 107658, 2021.
- [15] M. Ju, X. Li, X. Li, and G. Zhang, “A review of the effects of weak interfaces on crack propagation in rock: from phenomenon to mechanism,” *Engineering Fracture Mechanics*, vol. 263, Article ID 108297, 2022.
- [16] M. Ju and H. Xing, “Crack propagation in jointed rock and its effect on rock macrofracture resistance: insights from discrete element analysis,” *Geomechanics and Geophysics for Geo-Energy and Geo-Resources*, vol. 8, no. 1, pp. 21–22, 2022.
- [17] W. L. Tian, S. Q. Yang, J. G. Wang, and W. Zeng, “Numerical simulation of permeability evolution in granite after thermal treatment,” *Computers and Geotechnics*, vol. 126, Article ID 103705, 2020.
- [18] N. Liu, L. Peng, C. Shi, and M. Lei, “Experimental and model study on dynamic behaviour and fatigue damage of tunnel invert,” *Construction and Building Materials*, vol. 126, pp. 777–784, 2016.
- [19] L. Peng, C. Shi, J. Huang, and S. Liu, “Study on the fatigue life of the tunnel bed structure under train loads,” *Journal of the China Railway Society*, vol. 29, no. 1, pp. 82–85, 2007.
- [20] W. Yao, *Fatigue Life Prediction of Structures*, National Defence Industry Press, Beijing, China, 2003.
- [21] Y. Hu, “Current status and development trend of technology system for railway heavy haul transport in China,” *Journal of Vibration and Shock*, vol. 36, no. 2, pp. 1–10, 2015.
- [22] W. Yin and T. T. C. Hsu, “Fatigue behavior of steel fiber reinforced concrete in uniaxial and biaxial compression,” *ACI Materials Journal*, vol. 92, no. 1, pp. 71–81, 1995.
- [23] W. Cao, J. Hu, and Y. Song, “Analysis of the fatigue strength of concrete under multi-axial compressive cyclic loading,” *China Civil Engineering Journal*, vol. 38, no. 08, pp. 31–35, 2005.